First-principles calculations of ELNES and XANES of selected wide-gap materials: Dependence on crystal structure and orientation

Teruyasu Mizoguchi,[1,*] Isao Tanaka,[1,2] Satoru Yoshioka,[1] Masahiro Kunisu,[1] Tomoyuki Yamamoto,[2] and W. Y. Ching[3]
[1]*Department of Materials Science and Engineering, Kyoto University, Sakyo, Kyoto 606-8501 Japan*
[2]*Fukui Institute for Fundamental Chemistry, Kyoto University, Sakyo, Kyoto 606-8103 Japan*
[3]*Department of Physics, University of Missouri–Kansas City, Kansas City, Missouri 64110, USA*
(Received 5 December 2003; published 13 July 2004)

Theoretical calculations of electron energy-loss near-edge structure (ELNES) and x-ray absorption near-edge structure (XANES) of selected wide-gap materials including TiO_2, AlN, GaN, InN, ZnO, and their polymorphs are performed using a first-principles method. Calculations of 39 *K* and $L_3(L_{2,3})$ edges are made using large supercells containing 72 to 128 atoms. A core hole is included in the final state, and the matrix elements of the electric dipole transition between the ground state and the final state are computed. Structures of some metastable crystals are optimized by a plane-wave basis pseudopotential method. Spectral differences in ELNES and XANES among polymorphs are quantitatively reproduced in this way. The origin of the spectral differences is pursued from the viewpoint of chemical bondings. Crystallographic orientation dependence of ELNES and XANES is also examined both by experiment and theory. The dependence is found to be much larger in *K* edges than that in $L_3(L_{2,3})$ edges.

DOI: 10.1103/PhysRevB.70.045103 PACS number(s): 71.20.Nr, 78.70.Dm, 79.20.Uv, 82.80.−d

I. INTRODUCTION

Fine structures that appear in electron energy-loss near-edge structure (ELNES) and x-ray absorption near-edge structure (XANES) provide us information about electronic structure and chemical bonding around objective atoms in materials.[1,2] ELNES is equivalent to XANES when measured by an electron energy loss spectrometer (EELS) which is equipped with transmission electron microscopy (TEM) or scanning TEM (STEM). Employing modern TEM-EELS or STEM-EELS, an observation of edge structures with sub-eV resolution using subnano probe is possible.[3,4] Therefore, ELNES has the potential to identify electronic and bonding structures in nano or Å regions, such as atomic-scale thin films, nanoparticles, and grain boundaries. ELNES is used mainly on light elements, whereas XANES can be applied to most elements in the Periodic Table. Although XANES is inferior to ELNES in spatial resolution, it is superior in the lower detectable limit. By employing the third generation synchrotron facilities, XANES from ultradilute dopants of a few ppm level can be obtained with sufficient signal to noise ratio.[5] ELNES and XANES are therefore complementary tools for modern materials characterization.

In order to fully utilize ELNES and XANES, a good theoretical tool to interpret and reproduce the experimental spectra is essential. Efforts to reproduce ELNES and XANES have been made using several theoretical methods.[6–10] Cluster calculations on the basis of multiple scattering theory and molecular orbital theory have been successful for many molecular systems.[11,12] For crystalline systems, calculations imposing periodic boundary condition should be a natural way. However, reproduction of experimental spectra was not always satisfactory in such calculations. The major reason for the poor reproduction can be ascribed to the neglect of, or improper treatment of, a core hole associated with the electronic transition. Electronic wave functions of the unoccupied bands are significantly changed by the presence of the core hole.[13–15] Unless the core-hole effect is rigorously included, theoretical calculations can never reproduce the experimental spectra. It should also be emphasized that the use of a large supercell to minimize the interactions among core holes is essential. Since the use of a large supercell is computationally demanding, not many works have examined the size dependence seriously. An alternative approach to account for the core-hole effect is the Z+1 approximation in which the core-hole effects are introduced by increasing the atomic number (Z) by 1. Lie *et al.* succeeded in the reproduction of B-K ELNES from AlB_2 and TiB_2 using the Z+1 approximation.[16,17] But, one must realize that the Z+1 approximation is not always appropriate.[18,19] Nufer *et al.* reported the theoretical calculation of Al-K and Al-L_1 ELNES of Al_2O_3 using the Z+1 approximation.[18] They demonstrated that this approximation is not applicable to the L_1 edge. Even when the spectrum accidentally reproduces the experimental spectrum, estimation of the absolute transition energy is impossible by the Z+1 approximation.

Quantitative calculation of ELNES and XANES using the first-principles orthogonalized linear combinations of atomic orbitals (OLCAO) method was performed by Mo and Ching.[20] They introduce a core hole by removing one electron at a core orbital and putting one electron to the unoccupied band. The core-hole effect was thereby fully taken into account in their calculation. They pointed out that supercells with more than 100 atoms are generally required to minimize the artificial interactions among core holes. They together with our group have been using the OLCAO method to calculate ELNES and XANES of many systems and confirmed its validity and effectiveness.[5,20–24] Experimental spectra of all edges in many crystals have been well reproduced, which have motivated us to predict unknown ELNES and XANES prior to experimental measurements.

In this study, we systematically examine the differences in spectral shapes of a few polymorphs of five compounds, i.e., TiO_2, AlN, GaN, InN, and ZnO. The aim of this work is not only the prediction of the unknown ELNES and XANES, but also the understanding of the relationship between the spectral shape and chemical bondings among those polymorphs. Calculations were made for both K and $L_3(L_{2,3})$ edges. Theoretical spectra were compared with experimental spectra. Some of the newly measured spectra were reported in a systematic manner in the present study. Crystallographic orientation dependence of the spectra was examined for the wurtzite compounds. They were also compared with the experimental spectra reported in the present work.

II. METHODOLOGY

A. Computational procedure

Orthogonalized linear combinations of atomic orbitals (OLCAO) method was employed to predict and interpret ELNES and XANES. This is a first-principles band structure method based on the density functional theory (DFT) within the local density approximation (LDA).[25] Each atomic orbital is expressed as a sum of Gaussian-type orbitals. Core orbitals can be eliminated from the final secular equation by an orthogonalization process, which can significantly reduce the computational time for large complex system.

On the electron transition process associated with ELNES and XANES, an electronic hole at a core orbital is created, which is called a core hole. We have demonstrated that the inclusion of the core hole is indispensable to reproduce the experimental spectra.[13–15] Approximate approaches to introduce the core-hole effect are the Slater's transition method [26] and the Z+1 approximation.[27] In the former approach, a half hole is introduced in a core-orbital and placed in an unoccupied band. In the Z+1 approximation, the excited atom is replaced by the next element in the Periodic Table. In this study, the core-hole effect was fully taken into account in the self-consistent iterations by removing an electron at the core orbital and putting it at the lowest band. We use neither the Slater's transition method nor the Z+1 approximation. In order to introduce the core hole in the OLCAO method, the core states of the excited atom are excluded from the orthogonalized process. Both the final state and the ground state were calculated separately. Theoretical transition energy was evaluated as the difference in the total energy of the supercell at the ground state and the final state.

Since the electronic transition responsible for both ELNES and XANES follows the dipole selection rule, K and $L_3(L_{2,3})$ edges reflect the p- and (s+d)-partial density of state (PDOS), respectively. Therefore, PDOS has often been used to compare with experimental spectrum.[9,16–18] In this study, however, we have computed the transition matrix between the final state and the ground state for the theoretical spectrum. By calculating the transition matrix, the dipole selection rule is included automatically. Intensity of a peak (I) in ELNES and XANES is proportional to the transition matrix which is expressed as follows:

$$I \propto \sum_f |\langle f|\mathbf{P}|i\rangle|^2 \delta(\hbar\omega - E_f + E_i), \qquad (1)$$

where E_i and E_f are the orbital energies of the initial and final state, respectively. **P** is the momentum operator and $\hbar\omega$ is the transition energy. f and i represent wave functions at the final state and at the ground state, respectively.[20] In order to achieve a high resolution, eight k points in the reduced Brillouin zone of the supercell were employed in the spectral calculation. The calculated spectrum is broadening by a Gaussian function of FWHM=1 eV in order to compare with experiments.

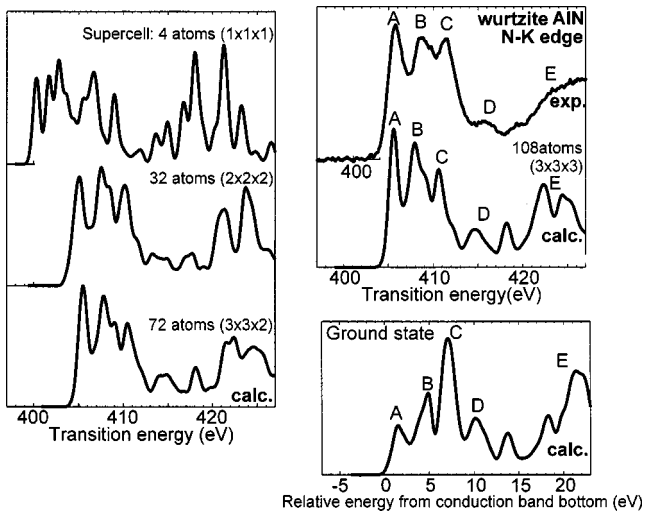

FIG. 1. Dependence on supercell size of N-K ELNES of wurtzite AlN. "Ground state" theoretical spectrum is made from the matrix elements between the core-orbital and unoccupied bands both at the ground state.

When we introduce the core hole in the band structure calculations, large supercells are indispensable to minimize the interactions among the core holes in the adjacent eells.[20,28] To demonstrate the importance of using a sufficiently large supercell, the size dependence on N-K ELNES of wurtzite-AlN is shown in Fig. 1. All spectra were calculated using the above method. Hereafter, the spectrum by Eq. (1) is called "spectrum at the final state" or simply "theoretical spectrum." A small supercell results in the inaccuracy of both the peak positions and relative intensities of the peaks. A supercell of more than 72 atoms is necessary to reproduce the experimental spectrum. The calculated spectrum at the ground state is also shown in the same figure. The "ground state" spectrum was obtained by calculating the transition matrix between the unoccupied bands and the core orbital both at the ground state. The spectrum at the ground state is far from being satisfactory in reproducing the experimental ELNES. In this study, we have employed 72- to 128-atom supercells in all calculations. Using such supercells, the distance of separation between the core-holed atoms in adjacent cells is approximately 10 Å.

In order to determine lattice constant for some metastable phases with no experimental data, the plane-wave basis pseudopotential (PWPP) method[29] was employed because of its efficiency and accuracy in structural optimization. Primitive cell was employed in the optimization process. Plane-wave cutoff energies were 380 eV for both oxides and nitrides. The optimization was truncated when the residual forces for the relaxed atoms were 0.05 eV/Å or less. The lattice parameters used in the present calculation are summarized in Table I.

TABLE I. Lattice parameters used in this work.

Rutile	Anatase	Brookite	Wurtzite	Zinc blende	Rock salt
	TiO_2			AlN	
exp.[a]	exp.[a]	exp.[b]	exp.[c]	exp.[d]	exp.[e]
a=4.594 Å	a=3.784 Å	a=9.184 Å	a=3.110 Å	a=4.439 Å	a=4.045 Å
c=2.959	c=9.515	b=5.447	c=4.980		
		c=5.145	u=0.382		
				GaN	
			exp.[f]	exp.[g]	calc.
			a=3.160	a=4.502	a=4.255
			c=5.125		
			u=0.375		
				InN	
			exp.[h]	exp.[i]	calc.
			a=3.537	a=4.980	a=4.712
			c=5.700		
			u=0.375		
				ZnO	
			exp.[j]	calc.	exp.[k]
			a=3.249	a=4.591	a=4.280
			c=5.205		
			u=0.383		

[a]Ref. 30.
[b]Ref. 31.
[c]Ref. 32.
[d]Ref. 33.
[e]Ref. 34.
[f]Ref. 35.
[g]Ref. 36.
[h]Ref. 37.
[i]Ref. 38.
[j]Ref. 39.
[k]Ref. 40.

B. Experimental procedure

The ELNES and XANES from wurtzite-AlN and -ZnO powder were systematically measured. Al-$L_{2,3}$, N-K, and O-K ELNES were recorded using transmission electron microscopy with a field emission gun (CM200FEG, FEI Company) with a CCD camera (GIF, Gatan Inc.) as a spectrum detector. Aperture size for the entrance of the spectrometer was 0.6 mm for Al-$L_{2,3}$ edge and 2.0 mm for both N-K and O-K edges. Energy resolution as measured by FWHM of the zero-loss peak was 0.8 and 1.0 eV for each aperture size, respectively. Although the energy drift was less than 1.0 eV/h, the energy calibration was made using the position of zero-loss peak which was recorded before and after the measurements.

Al-K and Zn-L_3 XANES were obtained at BL-1A and 7A in UVSOR at the Institute for Molecular Science, Okazaki, Japan. They were collected in the total electron yield mode at room temperature using a double-crystal monochromator of KTP and beryl, respectively. Samples were powdered and attached to the first photocathode of the electron multiplier by an adhesive carbon tape to minimize surface charging.

Zn-K XANES was observed at BL01B1 in SPring-8, Nishi-Harima, Japan. In order to achieve high-energy resolution, Si(311) double crystals were employed as a monochromator. Fluorescence x rays from a sample were detected using 19 sets of Ge solid state detectors. Dependence on the crystallographic orientation of XANES measured using a (0001) oriented wurtzite-ZnO thin film prepared by a pulsed laser deposition method on Al_2O_3(0001) substrate. The spectra were measured using a three-dimensional stage driven by stepping motors in order to optimize the sample position.

III. RESULTS AND DISCUSSION

A. O-K ELNES of TiO_2 polymorphs

Anatase, rutile, and brookite are well known polymorphs of TiO_2 that can be formed as minerals. Rutile and anatase have been extensively studied for their wide applications as photocatalysis[41,42] and gas sensor.[43] Coordination numbers for Ti and O in the three polymorphs are 6 and 3, respec-

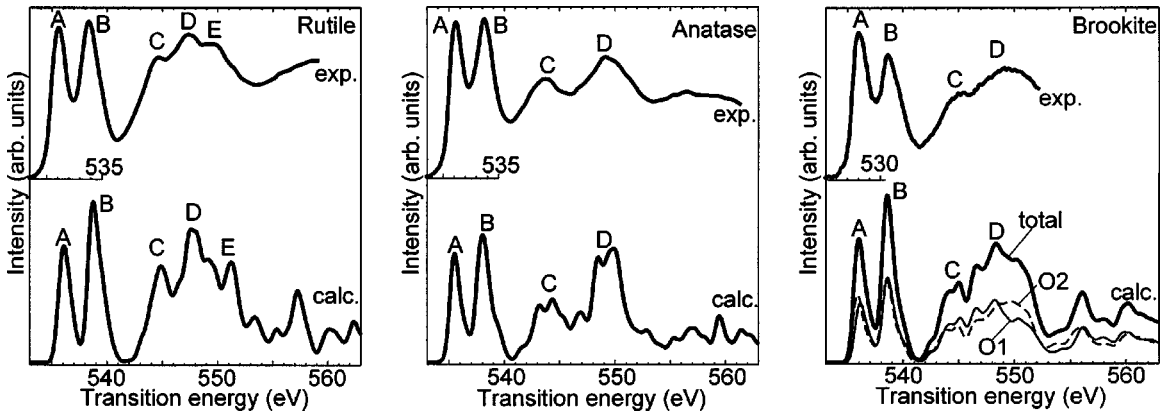

FIG. 2. Experimental and theoretical O-K ELNES for TiO_2 polymorphs, rutile, anatase, and brookite. Experimental spectra are from Refs. [6] and [45].

tively. Both rutile and anatase are tetragonal crystals in which two Ti-O bonds are longer than the other four Ti-O bonds. The distortion of the $[TiO_6]$ unit is greater in anatase than that in rutile. Two edges of the $[TiO_6]$ unit are shared in rutile, whereas four edges are shared in anatase. Some experimental and theoretical O-K ELNES of the two phases have been reported.[6,44] Brookite has a more complicated structure. The main difference from the other two phases is that there are six different Ti-O bond lengths in brookite. The structural distortion of the $[TiO_6]$ unit in brookite is greater than in other two phases. O-K ELNES of brookite have recently been reported by Lazar *et al.*[45]

Figure 2 shows O-K ELNES from the three TiO_2 polymorphs. Differences in O-K ELNES among the polymorphs appear in the region between 10 and 15 eV from the spectral onsets. O-K ELNES of rutile has three peaks C, D, and E, whereas anatase and brookite have two peaks C and D. The distance between peaks C and D in brookite is smaller than that in anatase. Below the experimental spectra, theoretical spectra were displayed. Supercell sizes of 72, 108, and 96 atoms were used for rutile, anatase, and brookite, respectively. Because brookite has two different oxygen sites both at the 8*c* site in Wyckoff's notation, they are labeled as O1 and O2. O-K ELNES from each site were independently calculated and the sum of the two is used as the theoretical spectrum. Spectral differences among the three polymorphs of TiO_2 are quantitatively reproduced by the theoretical spectra.[46]

B. ELNES and XANES of polymorphs for GaN, AlN, InN, and ZnO

Some nitrides and oxides with a wurtzite structure, such as GaN, AlN, InN, and ZnO, are wide gap materials that can be used for optelectronic applications. It is well known that these compounds transform to rock-salt structure under high pressures.[47] They also exhibit metastable zinc blende structure under appropriate growth conditions.[36,48–51] Properties of the wurtzite phase as well as their polymorphs have been extensively studied.[36,48–54] ELNES and XANES for the wurtzite phases have been reported by some researchers,[52–63] while only few experiments on the other polymorphs have been reported.[53] In particular, ELNES and XANES for the rock-salt phases have not been reported, to the authors' best knowledge. In this section, we report theoretical predictions of ELNES and XANES of the three polymorphs of GaN, AlN, InN, and ZnO. The calculated spectra of the wurtzite phase will be compared with experimental spectra. Comparison will be made for the other polymorphs whenever they are available. Relationship between chemical bondings and the spectral differences are discussed.

Structural difference between wurtzite and zinc blende structure is known to be small. The major one is the manner of layer stacking sequence. The wurtzite phase has A,B,A,B,…, stacking with a hexagonal unit cell, namely, 2H structure, whereas the zinc blende phase has A,B, C,A,B,C,…, stacking with a cubic unit cell, namely, 3C structure. The point symmetry of the tetrahedral unit $[AB_4]$ is also different. $[AB_4]$ in the wurtzite structure has a C_{3v} symmetry which is lower symmetry than that in the zinc blende structure T_d. The coordination number of all atoms in the two phases is 4, whereas in the rock-salt phase it is 6.

Figure 3 shows the N-K edges from wurtzite-GaN, -AlN, and -InN. Experimental spectra of the wurtzite-GaN and -InN have been reported by Chiou *et al.*[57] and Mkhoyan *et al.*,[56] respectively. Among the polymorphs, only the N-K ELNES of the zinc blende GaN have been reported by Katsikini *et al.*[53] Theoretical spectra for the wurtzite phase were obtained using 108-atom supercells. 128-atom supercells were employed for calculations in both the zinc blende and rock-salt phases. As can be seen from Fig. 3, experimental spectra of the wurtzite compounds are well reproduced by the calculated spectra. Spectral differences between wurtzite and zinc blende GaN are found at peaks C and D. Peak C is sharper, and peak D is less distinctive in the zinc blende phase. The small differences are also well reproduced by the present calculation.[64]

Although the calculated spectra of the wurtzite and zinc blende compounds look similar to each other, detailed inspection reveals that some of peaks in the zinc blende are sharper than that for the wurtzite phase, such as peaks C and E. The spectral difference results from the higher order of symmetry of the structural unit in the zinc blende phase. On the other hand, the calculated spectra from the rock-salt

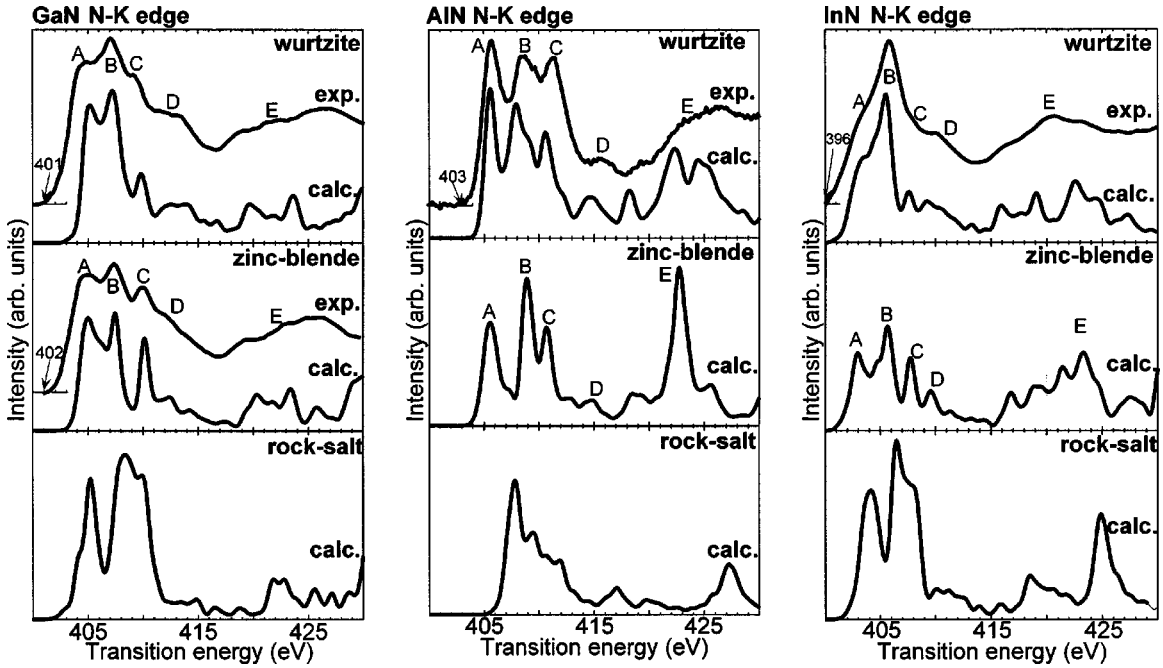

FIG. 3. Nitrogen K edges for the three polymorphs of GaN, AlN, and InN. Experimental spectra of wurtzite GaN, zinc blende GaN, and wurtzite InN are from Refs. [57,53], and [56], respectively. Values shown with an arrow at thresholds of experimental spectra refer to original values in experimental reports before alignment to the theoretical spectra.

structure are apparently different from that of the other phases. This can be ascribed to different coordination number of atoms in the rock-salt phases.

Figures 4 and 5 show cation $L_3(L_{2,3})$ edges and K edges from GaN, AlN, and InN. The magnitude of the splitting of L_2 and L_3 edges for Ga and In were reported to be 27 and 208 eV, respectively.[65] Spin-orbit coupling was not included in the present calculation. Experimental spectra of InN have not been reported. Experimental spectra from wurtzite GaN and AlN are well reproduced by the calculation.

The same trend of spectral difference among polymorphs as in N-K edges is found. Some of the peaks in the zinc

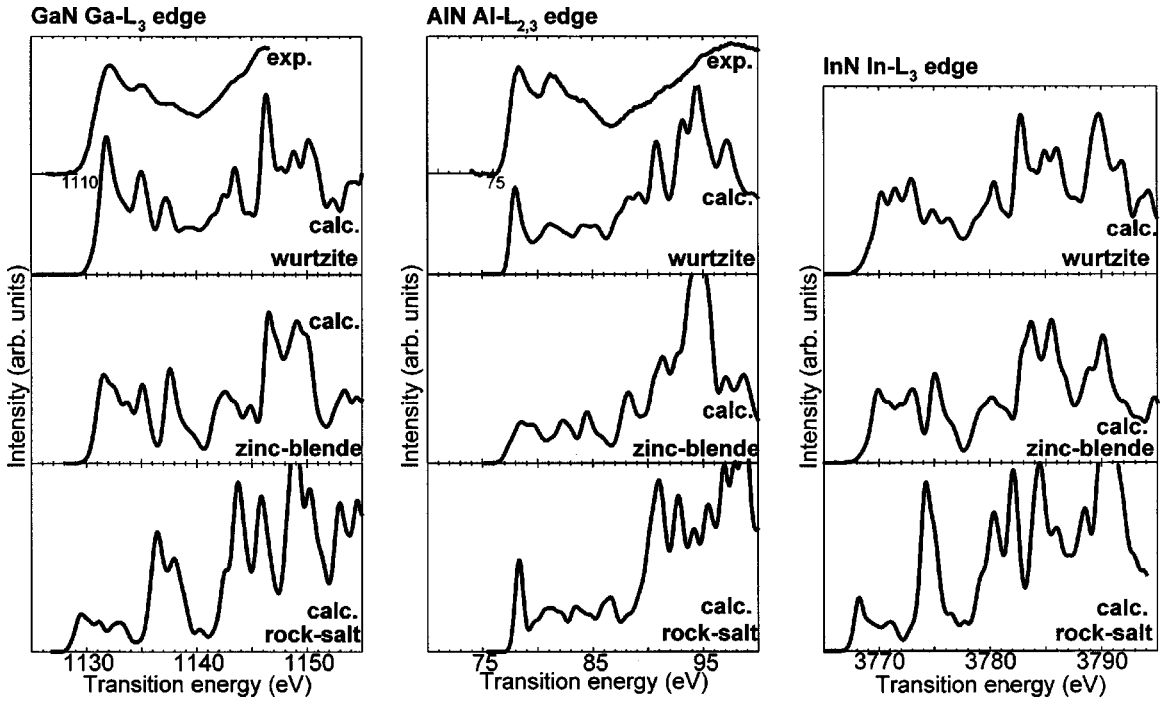

FIG. 4. Cation $L_3(L_{2,3})$ edges from three polymorphs of GaN, AlN, and InN. Experimental spectrum of L_3 edge of wurtzite GaN is from Ref. 57.

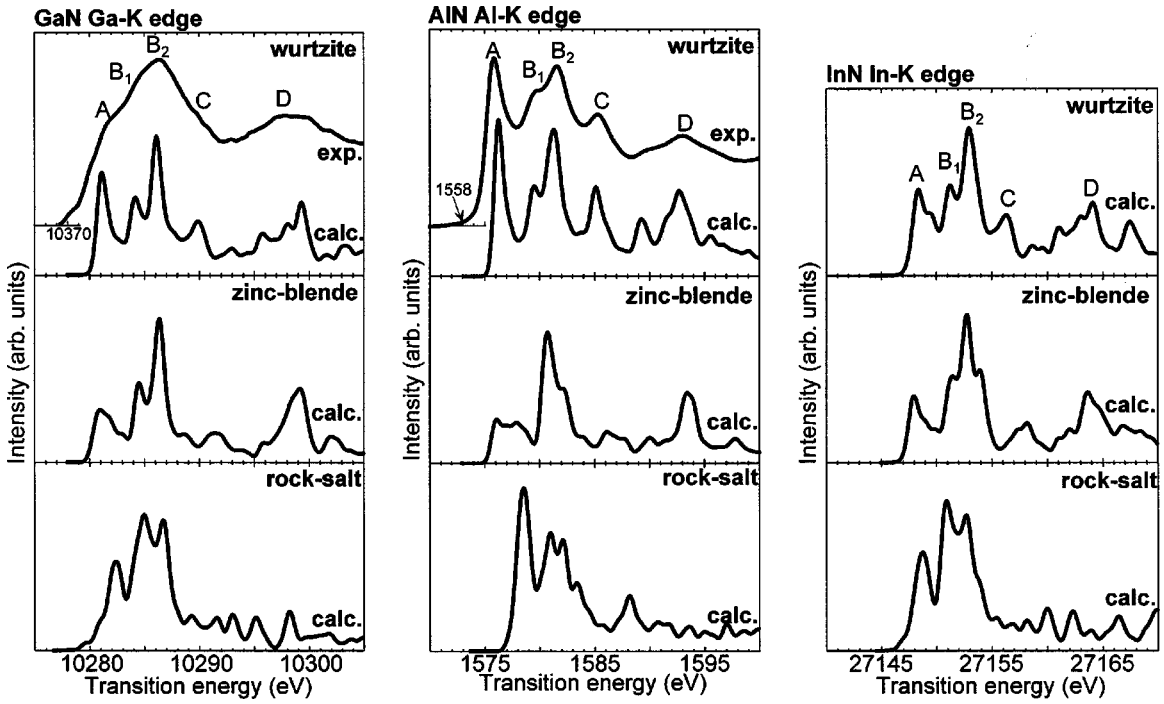

FIG. 5. Cation K edges for three polymorphs of GaN, AlN, and InN. Experimental spectrum of wurtzite GaN is from Ref. 57.

blende phases are sharper than that in the wurtzite phases, and spectral features in the rock-salt phases are different from those of other phases. However, the first peak in both K and $L_3(L_{2,3})$ edges of zinc blende is broader than that of wurtzite. In particular, the first peak becomes a doublet in the zinc blende AlN. This difference is contrary to the intuition that a structure with a higher symmetry should have simpler spectral feature. The origin of this broadening has been investigated in our previous work on the theoretical calculation of ELNES of AlN polymorphs. The doublet at the first peak is caused by the large hybridization of Al p orbitals with d orbitals.[24] In order to estimate the magnitude of the hybridization, net charges for the cations in the ground state were calculated by Mulliken population analysis and are listed in Table II. The net charges in the zinc blende phases were consistently lower than that in the wurtzite phases. This means cation-anion bonds are more covalent in the zinc blende phases. Assuming that the magnitude of p-d hybridization increases with covalency, this result suggests a greater p-d hybridization in zinc blende than in wurtzite. The difference between the two polymorphs is the largest in AlN, which results in the appearance of a clear doublet in AlN.

TABLE II. Net charge of the cation in each compound with wurtzite and zinc blende structures as evaluated by Mulliken population analysis by separated minimal basis-set calculations.

	wurtzite	zinc blende
Al in AlN	0.84	0.71
Ga in GaN	0.68	0.59
In in InN	0.66	0.58

Figure 6 shows ELNES and XANES of ZnO polymorphs. Only experimental spectra from the wurtzite phase are available. Calculations were performed using the same supercell sizes as in the nitrides. The spectral feature of Zn-L_3 XANES corresponds to our previous ELNES report.[66] The calculated spectra well reproduce the experimental spectra. The predicted spectrum for the zinc blende ZnO has a lot of similarity with that of the wurtzite ZnO. The predicted spectra for the rock-salt ZnO are clearly different from that of other polymorphs. These trends are similar to that for the nitrides.

C. Crystallographic orientation dependence of ELNES and XANES

In this section, we show dependence of ELNES and XANES on the crystallographic orientation. When materials possess anisotropy in their structure, many physical properties change with directions.[67–69] The change is caused by the anisotropy in the electronic structures. ELNES and XANES are effective tools to detect such anisotropy.[53,54,58–62] Among the polymorphs discussed in the previous section, the crystallographic orientation dependence of the ELNES and XANES can be expected only in the wurtzite phase because of its hexagonal lattice.

Figure 7 shows results for wurtzite-ZnO. Experimental Zn-K XANES was obtained using polarized x-rays of which the electric field is either parallel or perpendicular to the c axis of the (0001) oriented ZnO thin film. They were denoted by $c\|E$ and $C\perp E$, respectively. Theoretical spectra were obtained by resolving the transition matrix in the corresponding direction. The average of them $[2/3(c\perp E)+1/3(c\|E)]$ corresponds to the non polarized XANES shown in Fig. 6. It can be noted that peak B_1 and C in the nonpolarized Zn-K

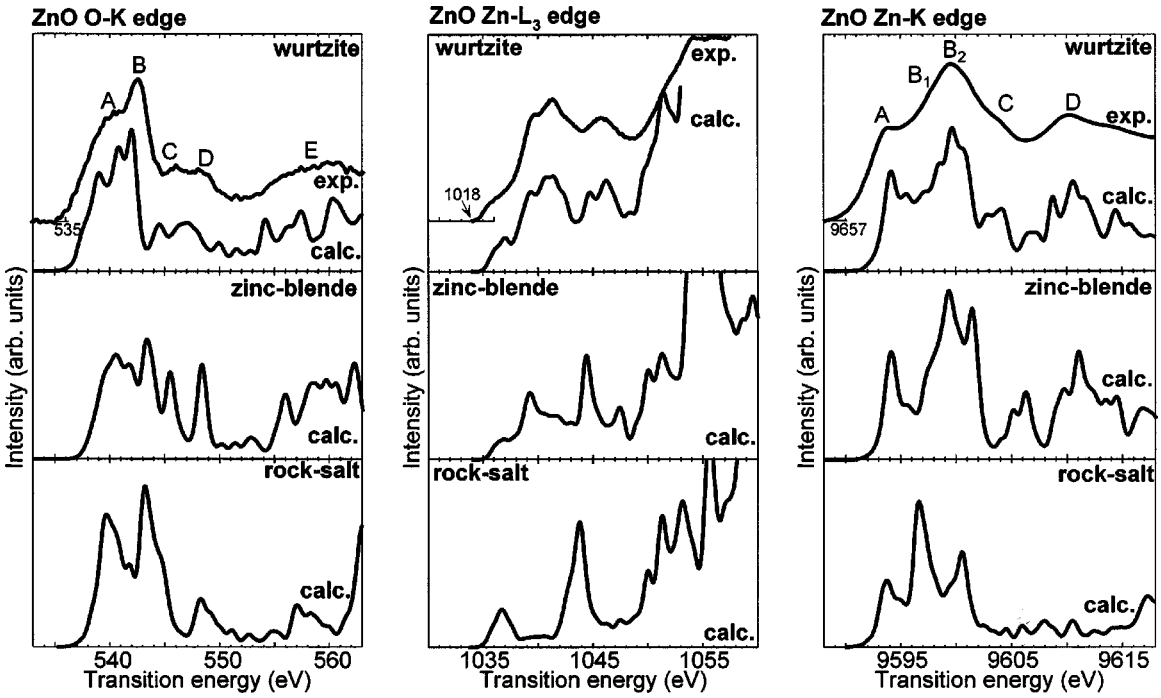

FIG. 6. Experimental and theoretical O-K, Zn-L_3, and Zn-K ELNES and XANES from wurtzite, zinc blende, and rock-salt-type ZnO.

XANES is mainly composed of the parallel components to the c axis, whereas peak B_2 is composed of the perpendicular components to the c axis. Clear crystallographic dependence can also be predicted for the O-K edge. Peaks C and D have their origins from the parallel and the perpendicular components, respectively. Contrary to those in K edges, the spectral changes due to the different incidence orientations are found to be small in the L_3 edge. The reason can be ascribed to different atomic orbitals that are responsible for K and L_3 edges. The K edge reflects mainly p-type orbitals, while L_3 edge reflects mainly s- and d-type orbitals. The s orbital is spherical. Empty 4d and 5d orbitals may not contribute much to the covalent bonding in those compounds. They are therefore less asymmetric.

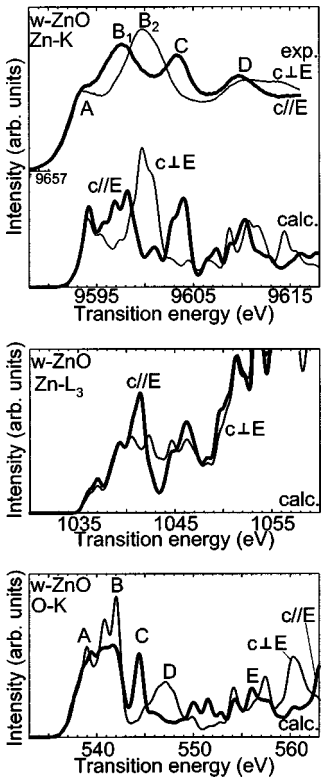

FIG. 7. Orientation dependence of Zn-K, Zn-L_3, and O-K ELNES and XANES of wurtzite ZnO. Thick and thin solid lines represent spectra for c∥E and c ⊥ E, respectively.

Figure 8 shows the spatially resolved results on the nitrides. Crystallographic orientation dependence of Ga-K XANES of wurtzite-GaN and N-K ELNES of wurtzite-AlN were reported by Pan *et al.*[62] and Radtke *et al.*,[58] respectively. The experimental spectra are well reproduced by the present calculations. Similar to the case of ZnO, spectral differences in polarized spectra for $L_3(L_{2,3})$ edges are predicted to be smaller than that for K edges. Peak B_1 and C in cation K edges of all compounds are due to the parallel components to the c axis, and peak B_2 is mainly composed of the perpendicular components to the c axis. Peak C and D in N-K edges of all compounds is composed of the parallel and perpendicular components to the c axis, respectively. The origin of each peak in those nitrides is the same as in the case of ZnO.

IV. SUMMARY

In this study, we have reported theoretical calculations of ELNES and XANES of TiO_2, AlN, GaN, InN, ZnO, and their polymorphs using first principles OLCAO method. All calculations were performed by using large supercells of 72 to 128 atoms. The effect of the core hole was fully taken into account by removing one electron at a core orbital and putting it to the empty band. Calculations of thirty-nine K and

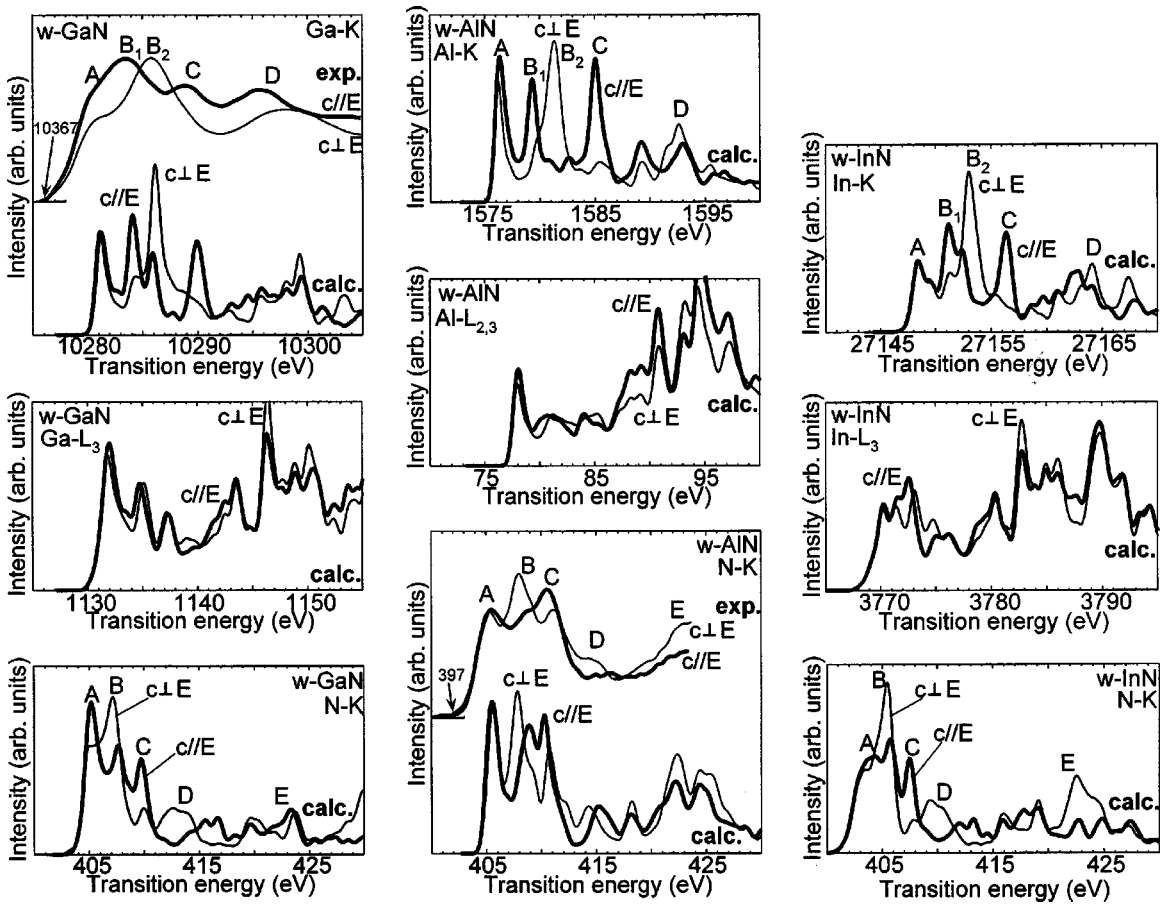

FIG. 8. Orientation dependence of ELNES and XANES for wurtzite GaN, AlN, and InN. The experimental Ga-K edge of GaN and N-K edge of AlN are from Refs. 62 and 58. Thick and thin solid lines represent spectra for c∥E and c ⊥ E, respectively.

$L_3(L_{2,3})$ edges were demonstrated. Results on this study are summarized as follows.

(1) By investigating the size dependence of the N-K ELNES of wurtzite-AlN, we found that a supercell size of more than 72 atoms is indispensable to treat the core hole adequately. Smaller cell size causes inaccuracy both in the peak positions and in the relative intensities of the peaks.

(2) O-K ELNES of the three TiO_2 polymorphs were quantitatively reproduced by the calculations. Spectral difference between wurtzite and zinc-blende phase was predicted to be small, whereas that of the rock-salt phase was large. Some peaks in the zinc-blende phase were predicted to be sharper than that in the wurtzite phase. This trend is natural because the zinc blende structure has a higher symmetry than the wurtzite structure. The first peak of cation K edges and $L_3(L_{2,3})$ edges were predicted to be broader in the zinc blende phase. This can be explained by the larger p-d hybridization in the zinc blende phase. Results of Mulliken population analysis were consistent with this idea.

(3) Crystallographic orientation dependence on the ELNES and XANES of the wurtzite compounds was investigated. Zn-K XANES was measured using the (0001) oriented wurtzite-ZnO thin film. The spectrum clearly changes depending upon the direction of the incident polarized x ray. Orientation dependence was found to be much larger in K edges as compared to the $L_{2,3}(L_3)$ edges. This trend can also be found in the other three nitrides.

In this paper, we have made a systematic study of a large number of ELNES and XANES spectra of several important oxides and nitrides. The results are extremely encouraging. The calculated spectra agree well with all measured spectra, thus give credence to the predicted spectra where measured data are unavailable. Furthermore, the anisotropic properties of the spectra can be predicted as well. The detailed spectral features can be interpreted with local bonding structure in a meaningful way. We are fully confident that this method can be effectively used as a major characterization tool for materials with even more complicated structures such as those found in grain boundaries, interfaces, and surfaces of these materials.

ACKNOWLEDGMENTS

T.M. is grateful to Dr. K. Matsunaga, Dr. T. Yamamoto, and Dr. Y. Ikuhara for their support at The University of Tokyo. The authors thank Dr. E. Shigemasa, Dr. N. Kondo, Dr. T. Okajima, Dr. M. Umesaki, Dr. T. Uruga, Dr. H. Tanida, and Dr. T. Homma for their help in experimental works at UVSOR and SPring-8. T.M. is supported by the Japan Soci-

ety for the Promotion of Science. This work was supported by three projects from the Ministry of Education, Culture, Sports, Science and Technology of Japan. They are Grant-in-Aid for Scientific Research on Priority Areas (Grant No. 751), the Computational Materials Science Project in Kyoto University, and the 21st century COE program. W.Y.C. was supported by the U.S. DOE under Grant No. DE-FG02-84-DR45170.

*Present address: Institute of Engineering Innovation, The University of Tokyo, Yayoi, Bunkyo, Tokyo 113-8656, Japan.

[1] J. Stöhr, *NEXAFS Spectroscopy* (Springer, Berlin, 1992).
[2] R. F. Egerton, *Electron Energy-loss Spectroscopy in the Electron Microscopy* (Plenum Press, New York, 1996).
[3] N. D. Browning, D. J. Wallis, P. D. Nellist, and S. J. Pennycook, Micron **28**, 333 (1997).
[4] D. A. Muller, T. Sorsch, S. Moccio, F. H. Baumann, K. Evans-Lutterodt, and G. Timp, Nature (London) **399**, 758 (1999).
[5] I. Tanaka, T. Mizoguchi, M. Matsui, S. Yoshioka, H. Adachi, T. Yamamoto, T. Okajima, M. Umesaki, W. Y. Ching, Y. Inoue, M. Mizuno, H. Araki, and Y. Shirai, Nat. Mater. **2**, 541 (2003).
[6] R. Brydson, H. Sauer, W. Engel, J. M. Thomas, E. Zeitler, N. Kosugi, and H. Kuroda, J. Phys.: Condens. Matter **1**, 797 (1989).
[7] X. Weng, P. Rez, and H. Ma, Phys. Rev. B **40**, 4175 (1989).
[8] P. Rez, J. Bruley, P. Brohan, M. Payne, and L. A. J. Garvie, Ultramicroscopy **59**, 159 (1995).
[9] S. Köstlemeier and C. Elsässer, Phys. Rev. B **60**, 14 025 (1999).
[10] P. Rez, J. R. Alvarez, and C. Pickard, Ultramicroscopy **78**, 175 (1999).
[11] H. Oji, R. Mitsumoto, E. Ito, H. Ishii, Y. Ouchi, K. Seki, T. Yokoyama, T. Ohta, and N. Kosugi, J. Chem. Phys. **109**, 10409 (1998).
[12] Y. Luo, H. Ågren, M. Keil, R. Friedlein, and W. R. Salaneck, Chem. Phys. Lett. **337**, 176 (2001).
[13] I. Tanaka and H. Adachi, Phys. Rev. B **54**, 4604 (1996).
[14] I. Tanaka, H. Araki, M. Yoshiya, T. Mizoguchi, F. Oba, and H. Adachi, Phys. Rev. B **60**, 4944 (1999).
[15] T. Mizoguchi, I. Tanaka, M. Yoshiya, F. Oba, K. Ogasawara, and H. Adachi, Phys. Rev. B **61**, 2180 (2000).
[16] K. Lie, R. Brydson, and H. Davock, Phys. Rev. B **59**, 5361 (1999).
[17] K. Lie, R. Høier, and R. Brydson, Phys. Rev. B **61**, 1786 (2000).
[18] S. Nufer, T. Gemming, C. Elsässer, S. Köstlemeier, and M. Rühle, Ultramicroscopy **86**, 339 (2001).
[19] S. Köstlemeier, Ultramicroscopy **86**, 319 (2001).
[20] S. D. Mo and W. Y. Ching, Phys. Rev. B **62**, 7901 (2000).
[21] S. D. Mo and W. Y. Ching, Appl. Phys. Lett. **78**, 3809 (2001).
[22] Y. N. Xu, Y. Chen, S. D. Mo, and W. Y. Ching, Phys. Rev. B **65**, 235105 (2002).
[23] W. Y. Ching, S. D. Mo, and Y. Chen, J. Am. Ceram. Soc. **85**, 11 (2002).
[24] T. Mizoguchi, I. Tanaka, M. Kunisu, M. Yoshiya, H. Adachi, and W. Y. Ching, Micron **34**, 249 (2003).
[25] W. Y. Ching, J. Am. Ceram. Soc. **73**, 3135 (1990).
[26] J. C. Slater, *Quantum Theory of Molecules and Solids* (McGraw-Hill, New York, 1974).
[27] T. Fujikawa, J. Phys. Soc. Jpn. **52**, 4001 (1983).
[28] C. Elsässer and S. Köstlemeier, Ultramicroscopy **86**, 325 (2001).
[29] M. D. Segall, P. J. D. Lindan, M. J. Probert, C. J. Pickard, P. J. Hasnip, S. J. Clark, and M. C. Payne, J. Phys.: Condens. Matter **14**, 2717 (2002).
[30] C. J. Howard, Z. M. Sabine, and F. Dickson, Acta Crystallogr., Sect. B: Struct. Sci. **47**, 462 (1991).
[31] V. Werner and H. Baur, J. Appl. Crystallogr. **14**, 214 (1961).
[32] H. Schult and K. Thiemann, Solid State Commun. **23**, 815 (1977).
[33] I. Petrov, E. Mojab, R. C. Powell, J. E. Greene, L. Hultman, and J.-E. Sundgren, Appl. Phys. Lett. **60**, 2491 (1992).
[34] H. Vollstädt, E. Ito, M. Akaishi, S. Akimoto, and O. Fukunaga, Proc. Jpn. Acad., Ser. B: Phys. Biol. Sci. **66**, 7 (1990).
[35] J. V. Lirman and G. S. Zhdanov, Acta Physicochim. URSS **6**, 306 (1937).
[36] H. Yamane, M. Shimada, and F. J. DiSalvo, Mater. Lett. **42**, 66 (2000).
[37] R. Juza and H. Aahn, Z. Anorg. Allg. Chem. **239**, 282 (1938).
[38] D. Chandrasekhar, D. J. Smith, S. Strite, M. E. Lin, and H. Morkoç, J. Cryst. Growth **152**, l35 (1995).
[39] S. C. Abrahams and J. L. Bernstein, Acta Crystallogr., Sect. B: Struct. Crystallogr. Cryst. Chem. **25**, 1233 (1969).
[40] C. H. Bates, W. B. White, and R. Roy, Science **137**, 993 (1962).
[41] R. Asahi, T. Morikawa, T. Ohwaki, K. Aoki, and Y. Taga, Science **239**, 269 (2001).
[42] S. J. Tauster, S. C. Fung, and R. L. Garten, J. Am. Ceram. Soc. **100**, 170 (1978).
[43] D. Kohl, Sens. Actuators **18**, 71 (1989).
[44] F. M. F. de Groot, J. Faber, J. J. M. Michiels, M. T. Czyżyk, M. Abbate, and J. C. Fuggle, Phys. Rev. B **48**, 2074 (1993).
[45] S. Lazar, G. A. Botton, M.-Y. Wu, F. D. Tichelaar, and H. W. Zandbergen, Ultramicroscopy **96**, 535 (2003).
[46] The experimental transition energy in brookite has been reported to be 5 eV lower than the other polymorphs. However, it may be caused by an experimental error because such a shift is not found in the present calculation.
[47] A. Mujica, A. Rubio, A. Muñoz, and R. J. Needs, Rev. Mod. Phys. **75**, 863 (2003).
[48] I. W. Kim, A. Madan, M. W. Guruz, V. P. Dravid, and S. A. Barnett, J. Vac. Sci. Technol. A **19**, 2069 (2001).
[49] I. Petrov, E. Mojab, R. C. Powell, J. E. Greene, J. Hultman, and J.-E. Sundgren, Appl. Phys. Lett. **60**, 2491 (1992).
[50] J. Šik, M. Schubert, G. Leibiger, V. Gottschalch, and G. Wagner, J. Appl. Phys. **89**, 294 (2001).
[51] C.-Y. Yeh, Z. W. Lu, S. Froyen, and W. Zunger, Phys. Rev. B **46**, l0 086 (1992).
[52] D. Fritsch, H. Schmidt, and M. Grundmann, Phys. Rev. B **67**, 235205 (2003).
[53] M. Katsikini, E. C. Pauloura, and T. D. Moustakas, Appl. Phys. Lett. **69**, 4206 (1996).
[54] M. Katsikini, E. C. Pauloura, and T. D. Moustakas, J. Appl. Phys. **83**, 1437 (1998).
[55] M. Katsikini, E. C. Pauloura, J. Antonopoulos, P. Bressler, and T.

D. Moustakas, J. Cryst. Growth **230**, 405 (2001).
[56] K. A. Mkhoyan, J. Silcox, E. S. Alldredge, N. W. Ashcroft, H. Lu, W. J. Schaff, and L. F. Eastman, Appl. Phys. Lett. **82**, 1407 (2003).
[57] J. W. Chiou, J. C. Jan, H. M. Tsai, W. F. Pong, M.-H. Tsai, I.-H. Hong, R. Klauser, J. F. Lee, C. W. Hsu, H. M. Lin, C. C. Chen, C. H. Shen, L. C. Chen, and K. H. Chen, Appl. Phys. Lett. **82**, 3949 (2003).
[58] G. Radtke, T. Epicier, P. Bayle-Guillemaud, and J. C. Le Bossé, J. Microsc. **210**, 60 (2003).
[59] I. J. Lee, H. J. Shin, S. S. Chang, M. K. Lee, and H. K. Kim, Appl. Phys. Lett. **82**, 2981 (2003).
[60] M. Lübbe, P. R. Bressler, W. Braun, T. U. Kampen, and D. R. T. Zahn, J. Appl. Phys. **86**, 209 (1999).
[61] F. d'Acapito, F. Bosherini, S. Mobilio, A. Rizzi, and R. Lantier, Phys. Rev. B **66**, 205411 (2002).
[62] Y. C. Pan, S. F. Wang, W. H. Lee, M. C. Lee, W. K. Chen, W. F. Chen, L. Y. Jang, J. F. Lee, C. I. Chiang, H. Cang, K. T. Wu, and D. S. Lin, Appl. Phys. Lett. **78**, 31 (2001).
[63] V. Serin, C. Colliex, R. Brydson, S. Matar, and F. Bousher, Phys. Rev. B **58**, 5106 (1998).
[64] Transition energy difference of 1 eV between wurtzite and zinc blende was found in experiment, while it was not observed in the present theoretical spectra. Katsikini *et al*. have also reported N-K XANES from both polymorphs in Ref. 53. Although they have reported the spectrum only with special directions of incidence, such an energy shift was not found in their results.
[65] J. A. Beaurden and A. F. Burr, Rev. Mod. Phys. **39**, 125 (1967).
[66] T. Mizoguchi, M. Yoshiya, J. Li, F. Oba, I. Tanaka, and H. Adachi, Ultramicroscopy **86**, 363 (2001).
[67] C. C. Chen, K. L. Hsieh, J. K. Sheu, G. C. Chi, M. J. Jou, C. H. Lee, and M. Z. Lin, Appl. Phys. Lett. **79**, 1477 (2001).
[68] R. Zhang, B. Jiang, and W. Cao, Appl. Phys. Lett. **82**, 3737 (2003).
[69] N. Mochida, T. Honda, T. Shirasawa, A. Inoue, T. Sakaguchi, F. Koyama, and K. Iga, J. Cryst. Growth **189**, 716 (1998).